Catalytic Properties of Botulinum Neurotoxin Subtypes A3 and A4[†]

James S. Henkel,[‡] Mark Jacobson,[§] William Tepp,[§] Christina Pier,[§] Eric A. Johnson,[§] and Joseph T. Barbieri*[,‡]

Microbiology and Molecular Genetics, Medical College of Wisconsin, Milwaukee, Wisconsin 53226, and Department of Bacteriology, University of Wisconsin, Madison, Wisconsin 53706-1521

Received September 4, 2008; Revised Manuscript Received December 30, 2008

ABSTRACT: Botulinum toxins (BoNT) are zinc proteases (serotypes A−G) which cause flaccid paralysis through the cleavage of SNARE proteins within motor neurons. BoNT/A was originally organized into two subtypes, BoNT/A1 and BoNT/A2, which are ∼95% homologous and possess similar catalytic activities. Subsequently, two additional subtypes were identified, BoNT/A3 (Loch Maree) and BoNT/A4 (657Ba), which are 81 and 88% homologous with BoNT/A1, respectively. Alignment studies predicted that BoNT/A3 and BoNT/A4 were sufficiently different from BoNT/A1 to affect SNAP25 binding and cleavage. Recombinant light chain (LC) of BoNT/A3 (LC/A3) and BoNT/A4 (LC/A4) were subjected to biochemical analysis. LC/A3 cleaved SNAP25 at 50% of the rate of LC/A1 but cleaved SNAPtide at a faster rate than LC/A1, while LC/A4 cleaved SNAP25 and SNAPtide at slower rates than LC/A1. LC/A3 and LC/A4 had similar K_m values for SNAP25 relative to LC/A1, while the k_{cat} for LC/A4 was 10-fold slower than that for LC/A1, suggesting a defect in substrate cleavage. Neither LC/A3 nor LC/A4 possessed autocatalytic activity, a property of LC/A1 and LC/A2. Thus, the four subtypes of BoNT/A bind SNAP25 with similar affinity but have different catalytic capacities for SNAP25 cleavage, SNAPtide cleavage, and autocatalysis. The catalytic properties identified among the subtypes of LC/A may influence strategies for the development of small molecule or peptide inhibitors as therapies against botulism.

The *Clostridium botulinum* neurotoxins (BoNTs)[1] are the most toxic proteins for humans and have been characterized as Category A agents by the Center for Disease Control and Prevention. BoNTs block neurotransmitter signal transduction in motor neurons, causing flaccid paralysis (*1*). This inhibition occurs through the cleaving of SNARE proteins that function in synaptic vesicle exocytosis (*1, 2*). Conversely, BoNTs are among the most useful reagents for treating neuromuscular afflictions (*3*).

Clostridia produce BoNTs as single-chain, 150 kDa proteins, which are cleaved into dichain proteins that are linked by a disulfide bond with **AB** structure function properties (*4*). The N-terminal **A** domain (light chain, LC) is an ∼50 kDa zinc metalloprotease with the characteristic thermolysin family zinc coordination motif (HExxH) (*1*). The C-terminal **B** domain (heavy chain, HC) is ∼100 kDa and is composed of two functional domains that are involved in receptor recognition (HCR) and translocation of the LC across the endosomal membrane (HCT) (*4*). Antibody neutralization differentiates BoNTs into seven serotypes, A−G. BoNTs share ∼65% primary amino acid similarity and ∼35% amino acid identity with tetanus toxin (*5*) and cleave different SNARE proteins: SNAP25 for A, C, and E; Syntaxin 1a for C; and VAMP-2 for B, D, F, G, and tetanus toxin (*2, 6, 7*). Cleavage sites within each SNARE substrate differ among the various neurotoxins, suggesting specific residues on the LC are necessary for recognition of substrate. Recent studies have identified residues necessary for substrate recognition by LC/A, LC/B, LC/D, LC/F, and tetanus toxin (*8*−*17*), mechanistically supporting a crystal structure of a noncatalytic LC/A bound to SNAP25 through exosite and active site interactions (*11, 12, 17*). BoNT serotypes also comprise subtypes that can vary between 3 and 32% at the primary amino acid level (*18*). BoNT/A1 and BoNT/A2 show similar cleavage of SNAP25 and possess ∼95% primary amino acid homology (*19*). Recent DNA sequencing analyses revealed two additional subtypes of BoNT/A, BoNT/A3 and BoNT/A4 (*19, 20*). The bacterium producing BoNT/A3 was isolated from a botulism outbreak in Scotland in 1922, while the bacterium producing BoNT/A4 was isolated from a case of infant botulism in 1988 (*21, 22*). LC/A3 is 81% identical to LC/A1, while LC/A4 is 88% identical to LC/A1 (*19*). The HCs of the subtypes of BoNT/A are ∼87% identical, and polyclonal antisera to BoNT/A1 neutralize BoNT/A2 (*18, 23*); however, there are sufficient amino acid differences that neutralizing monoclonal antibodies against BoNT/A1 are not effective in neutralizing BoNT/A2 (*18*). Previous modeling studies suggested that LC/A3 and LC/A4 may possess different catalytic activities for SNAP25 relative to LC/A1 (*19*). This study reports the catalytic properties of LC/A3 and LC/A4.

[†] This work was sponsored by the NIH/NIAID Regional Center of Excellence for Biodefense and Emerging Infectious Diseases Research (RCE) Program, Region V Great Lakes' RCE (NIH Grant 1-U54-AI-057153).

* To whom correspondence should be addressed. Phone: (414) 456-8412. Fax: (414) 456-6535. E-mail: jtb01@mcw.edu.

[‡] Medical College of Wisconsin.

[§] University of Wisconsin.

[1] Abbreviations: BoNT, botulinum neurotoxin; LC, light chain; HC, heavy chain; FRET, fluorescence resonance energy transfer; CD, circular dichroism.

10.1021/bi801686b CCC: $40.75
Published on Web 03/03/2009

EXPERIMENTAL PROCEDURES

Plasmid Construction and Protein Expression. Plasmids containing the full-length (1−448) light chain (LC) for LC/A1, LC/A2, LC/A3, and LC/A4 were obtained from E. Johnson (Madison, WI). Primers were designed for PCR amplification of DNA encoding amino acids 1−425 of LC/A2, LC/A3, and LC/A4, which has proved to be an optimal form of LC/A1 for structure−function studies (*24*). Amplified products were subcloned into pET-15b, to generate His_6-LC/A(1−425). A point mutation was engineered into LC/A4 at residue 264 by replacing Iso with Arg (I264R), using the Quikchange reaction (Stratagene) as described by the manufacturer. The mutated plasmid was transformed into *Escherichia coli* TG-1 and sequenced for mutation confirmation.

pET-15b containing LC/A1, LC/A2, LC/A3, LC/A4, or LC/A4-I264R was transformed into *E. coli* BL-21 RIL(DE3) (Stratagene). LC/A1, LC/A2, and LC/A3 were purified as previously described (*24*). Briefly, bacterial lawns were grown overnight on LB agar with 100 μg/mL ampicillin and 50 μg/mL chloramphenicol and then inoculated into 400 mL cultures of LB (six times, 400 mL cultures). Cultures were incubated at 30 °C for 2 h at 250 rpm, induced with 0.25 mM IPTG, and incubated at 16 °C overnight at 250 rpm. Cultures were centrifuged at 5000*g* for 10 min; the pellet was suspended in binding buffer, and bacteria were lysed using a French press (two times). The lysate was centrifuged at 27000*g* for 20 min at 4 °C (percent soluble LC determined at this point) and purified as a His_6 fusion protein on a Ni^{2+}-agarose (NiNTA) column (Qiagen), followed by size exclusion chromatography [Sephacryl S200 HR; 150 mL column equilibrated in 10 mM Tris-HCl (pH 7.6) with 20 mM NaCl]. Peak fractions were subjected to anion exchange chromatography [DEAE-Sephacel; 5 mL column, equilibrated in 10 mL of 10 mM Tris-HCl (pH 7.6) with 20 mM NaCl] and eluted with a gradient (from 20 to 750 mM NaCl) (yield of LC determined). LC/A4 and LC/A4-I264R were purified as described above without utilizing anion exchange chromatography (yield of LC determined). After dialysis, glycerol was added to a final concentration of 45% (v/v), and proteins were stored at −20 °C.

Protease Activity Assays. Reactions were conducted in 20 μL volumes. For substrate specificity, 0.2 μM LC/A was incubated with 3 μM SNAP25(141−206)-HA or SNAP25(141−206)-R198A-HA in 10 mM Tris (pH 7.6) and 20 mM NaCl for 1 h at 37 °C. The reaction was stopped with an equal volume of protein loading buffer, and the reaction product was separated from the substrate by 12% SDS−PAGE and detected by Coomassie staining. For the linear velocity, serially diluted LCs (from 2 μM to 5 nM) were incubated with 6 μM SNAP25(141−206) in 10 mM Tris (pH 7.6) and 20 mM NaCl at 37 °C for 15 min. The reaction was analyzed as described above and quantified by densitometry (AlphaEaseFC, Alpha Innotech). Kinetic constants for LC/A forms were determined in a reaction with increasing concentrations (0.015−120 μM) of SNAP25(141−206)-HA incubated for 15 min at 37 °C. Reactions were conducted in accordance with Michaelis−Menten reaction kinetics. Kinetic parameters were determined utilizing nonlinear regression equations using GraphPad Prism 5.00 (GraphPad Software, Inc.). Reactions were run three or more times and averaged for statistical error. For autocleavage of LC/A, the subtypes of LC/A (120 μM) were incubated in 10 mM Tris-HCl (pH 7.6) with 20 mM NaCl for timed intervals at 37 °C. The reaction mixture was subjected to SDS−PAGE, and cleavage products were detected by Coomassie staining. For the SNAPtide cleavage assay, LC/A was incubated with 5 μM SNAPtide (List Biologics) in 10 mM Tris-HCl (pH 7.6) with 20 mM NaCl (total reaction volume of 100 μL). Reactions were run in 96-well, clear-bottom plates at 37 °C in a Victor 3V fluorescence plate reader (Perkin-Elmer) with excitation at 488 nm and emission read at 523 nm at 2.5 min intervals. Fluorescent signals were subtracted from background fluorescence and then plotted as fluorescent units (arbitrary units) versus time for LC/A and recorded as relative fluorescent units per minute per nanomole of LC.

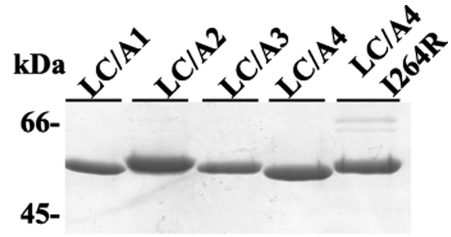

FIGURE 1: Purification of LC/A subtypes. LC/A subtype recombinant, purified proteins (3 μg) were subjected to 12% SDS−PAGE and visualized with Coomassie Brilliant Blue (shown).

Circular Dichroism (CD) Spectroscopy. LC/A subtypes were dialyzed into 10 mM $NaPO_4$ and 20 mM NaCl (pH 7.6) and subjected to CD analysis (10 mm cuvette, from 250 to 190 nm at a 0.5 nm data pitch, Jasco circular dichroism spectrometer). Samples were scanned at least 10 times to obtain an average, and data were plotted using GraphPad 5.00.

Trypsin Digestion Assay. LC/A subtypes (amount or concentration) were incubated in 10 mM Tris-HCl (pH 7.6) with 20 mM NaCl (volume) for the indicated times (0−20 min) at 37 °C alone or with 20 nM porcine trypsin (Sigma-Aldrich). The reaction was stopped with SDS−PAGE sample buffer and the mixture subjected to SDS−PAGE. Cleavage products were detected by Coomassie staining.

RESULTS

Production of LC/A3 and LC/A4 in E. coli. DNA encoding LC/A3(1−425) and LC/A4(1−425) were subcloned into pET-15b and expressed as His_6 fusion proteins, which migrated via SDS−PAGE as ~50 kDa proteins. Approximately 85% of LC/A3 was produced as a soluble protein, while <10% of LC/A4 was soluble. The amount of culture used for the LC/A4 purification was increased to obtain sufficient soluble LC/A4 for characterization. Purification of LC/A3 yielded ~1.5 mg and a purity of 79%, while LC/A4 yielded ~0.5 mg from the soluble fraction and a purity of 78% (Figure 1). The insolubility of LC/A4 was unexpected, since LC/A4 shared ~88% primary amino acid homology with LC/A1 (*19*). A Kyte−Doolittle plot of the primary amino acid sequences predicted two differences in hydrophobicity between LC/A1 and LC/A4, which lay within the "250 loop", where LC/A1 has a Leu at residue 260 and an Arg at residue 264 and LC/A4 has Phe and Iso, respectively (Kyte and Doolittle mean hydrophobicity profile, Bioedit version 7.0.4.1) (Figure 2A,B). A point mutation changing Leu 260 to Phe (LC/A4-L260F) did not change

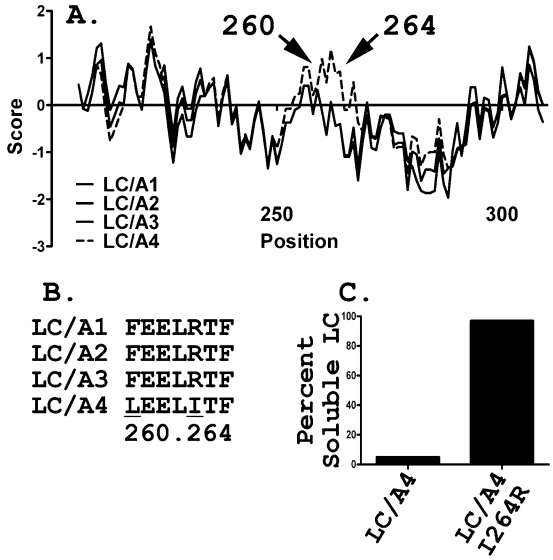

FIGURE 2: Solubility of LC/A4. (A) Kyte and Doolittle mean hydrophobicity profile of LC/A1−4. Arrows indicate residue substitutions causing a calculated increase in hydrophobicity locally: LC/A1, LC/A2, LC/A3 (—), and LC/A4 (---). Alignment and hydrophobicity plot calculated using BioEdit. Data for LC/A1−3 were plotted as solid lines due to their overlapping sequence. (B) LC/A subtype alignment of residues within the solubility pocket of LC/A4 (residues 260 and 264). Underlined lettering indicates residue substitution. (C) Quantification of LC/A4 and LC/A4-I264R solubility upon induction, lysis, and centrifugation as measured by densitometry of a Coomassie-stained, 12% SDS−PAGE gel.

the solubility (data not shown), while the Iso 264 to Arg (LC/A4-I264R) mutation was more soluble than LC/A4, approaching the solubility of LC/A1, when expressed in *E. coli* (Figure 2C).

SNAP25 Cleavage by LC/A3 and LC/A4. The four LC/A subtypes cleaved SNAP25 with LC/A4 less efficiently than the other LC/A subtypes (Figure 3A,C). Neither LC/A3 nor LC/A4 cleaved SNAP25-R198A, a P1′ mutated form of SNAP25 that abrogates cleavage by LC/A1 (Figure 3B). This indicated that LC/A3 and LC/A4 possessed the same cleavage site specificity for SNAP25 as LC/A1. In a linear velocity assay (Table 1), LC/A2 had the same activity as LC/A1, LC/A3 was ~2-fold less active than LC/A1, and LC/A4 was ~23-fold less active than LC/A1. LC/A4-I264R was ~10-fold more active than LC/A4, approaching the activity of LC/A3. Addition of 50 μM zinc did not increase the activity of LC/A3 or LC/A4 for SNAP25 cleavage, indicating that the lower catalytic rate was not due to nonoccupancy of zinc in the catalytic site (data not shown).

Experiments were also performed to determine the relative activity of native BoNT/A4. Although a limited amount of BoNT/A4 in the culture supernatant of the dual toxin producing *Clostridium* strain 657 Ba has prevented purification of BoNT/A4 from BoNT/B, Western blotting with α-LC/A IgG determined that partially purified Ba toxin preparations contained 0.1 pmol of BoNT/A4/μL. In an overnight assay, 0.01 pmol of LC/A1 cleaved 25% of the available SNAP25, while 0.1 pmol of BoNT/A4 did not yield detectable cleavage of SNAP25 [<2% cleavage, the limit of resolution (data not shown)]. Controls showed that BoNT/B in the partially purified toxin preparation cleaved VAMP under standard assay conditions (*25*), indicating that the partial purification did not intrinsically inactivate the

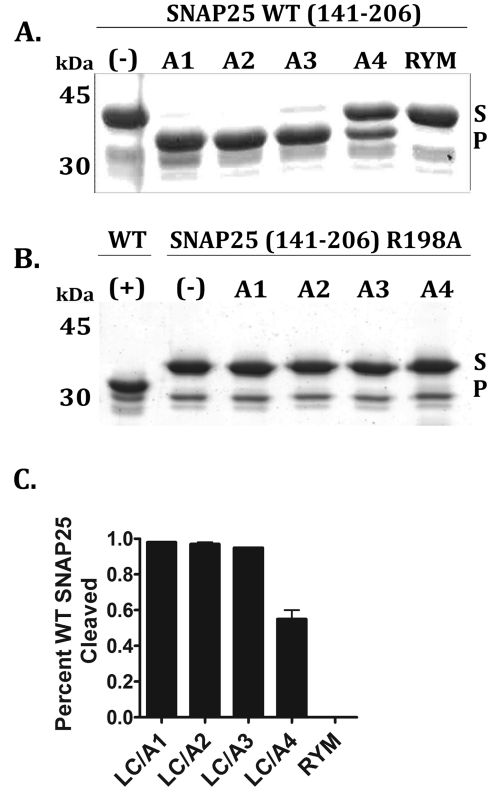

FIGURE 3: Cleavage site identification of LC/A subtypes. GST-SNAP25(141−206) (A) or GST-SNAP25(141−206-R198A) (B) (5 μM) was incubated with the indicated LC subtype (A1−4) at 0.2 μM and a noncatalytic LC control (RYM, LC/A1-R363A,Y366F) for 1 h at 37 °C. Reaction mixtures were subjected to SDS−PAGE (shown), and the amount of cleaved GST-SNAP25(141−206) was determined by densitometry of a Coomassie-stained gel (C). Error bars represent the average of at least three independent experiments. In panels A and B, the SNAP25 (substrate) and cleaved product (product) are indicated with arrows, S denotes the substrate, and P denotes the product band.

Table 1: Linear Velocity and SNAPtide Cleavage by LC/A Derivatives

LC/A	linear velocity[a] (relative velocity, 1 = LC/A1)	SNAPtide[b] (relative velocity, 1 = LC/A1)
LC/A1	1	1
LC/A2	0.92	18
LC/A3	0.52	49
LC/A4	0.04	0.01
LC/A4-I264R	0.38	2.9

[a] In the linear velocity assay, 2-fold dilutions of LC/A subtypes were incubated with GST-SNAP25 as described in Materials and Methods. Percent cleavage was determined by densitometry. The comparative activity was determined by the concentration of LC necessary for 20% substrate cleavage and expressed as a ratio of activity relative to that of LC/A1. Values are an average of at least three individual experiments with an error of ±4%. [b] For LC/A subtype cleavage of a fluorescence energy transfer (FRET) synthetic peptide substrate, SNAPtide (List Biologics), fluorescent signals were subtracted from background fluorescence and then plotted as fluorescent units (arbitrary units) vs time for LC/A subtypes. LC/A1 was determined to have a relative initial velocity [fluorescence units ($\times 10^6$) per minute per nanomoles of LC]. Values demonstrate the fold change from LC/A1 initial velocity (LC/A1 initial velocity = 1). Values were determined from a single representative experiment performed three independent times.

toxins. This is consistent with the native BoNT/A4 possessing a limited capacity to cleave SNAP25 relative to the A1 serotype.

Secondary Structure Analysis of LC/A4 and LC/A4-I264R. Improper protein folding could be responsible for the lower

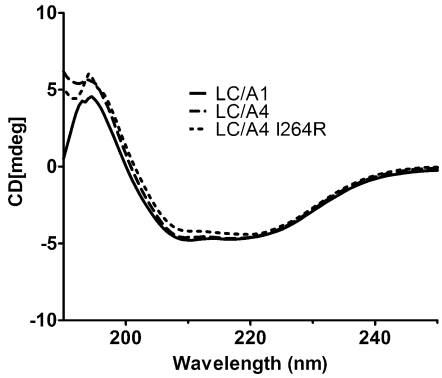

FIGURE 4: Structural folding of LC/A4. Circular dichroism (CD) spectroscopy of LC/A4 derivatives. LC/A1 (—), LC/A4 (---), and LC/A4-I264R (•••) were examined by CD at equimolar concentrations. Data represent an average of at least 10 independent scans.

Table 2: Kinetics of SNAP25 Cleavage by LC/A Derivatives[a]

enzyme	K_m (μM)	k_{cat} [nmol min^{-1} (nmol of LC)$^{-1}$]	k_{cat}/K_m
LC/A1	25 ± 7.5	10.7 ± 1.4	0.44
LC/A3	26 ± 6.8	9.3 ± 1.0	0.34
LC/A4	37 ± 9.4	0.13 ± 0.01	0.003
LC/A4-I264R	46 ± 9.6	5.2 ± 0.5	0.11

[a] LC/A1, LC/A3, LC/A4, and LC/A4-I264R were incubated with SNAP25(141−206) (1.25−80 μM) for 10 min at 37 °C. Reaction mixtures were then examined via SDS−PAGE, Coomassie-stained gels for cleavage and quantified by densitometry. Kinetic parameters were determined utilizing nonlinear regression equations on GraphPad Prism 5.00 (GraphPad Software, Inc.). Values were determined at a point where the level of substrate cleavage was <10% and are the average of three independent experiments.

catalytic activity of LC/A4, which was addressed by measuring the CD spectra of LC/A4 and LC/A4-I264R relative to that of LC/A1. The spectra showed similar β-strand content for the three proteins, while the α-helical content of LC/A4 was intermediate between those of LC/A4-I264R and LC/A1. The data indicated that the majority of LC/A4 was folded relative to LC/A4-I264R and LC/A1, and the difference in secondary structure content could not explain the low LC/A4 catalytic activity (Figure 4). Analysis of trypsin susceptibility showed that LC/A4, LC/A4-I264R, and LC/A1 had similar tryptic digestion patterns, also indicating that the overall structure of LC/A4 was similar to that of the catalytically active LCs (data not shown). This suggested that improper protein folding was not responsible for the observed differences in catalytic activity and that more subtle changes in the active site of LC/A4 were responsible for the lower observed activity. This also indicated that the increased activity of the I264R mutation within LC/A4 had a more direct effect on catalysis than could be explained by global folding effects.

Kinetic Properties of the LC for SNAP25 Cleavage. Kinetic constants of the LCs for SNAP25 cleavage were determined with Michaelis−Menten kinetic parameters. LC/A3 had k_{cat} and K_m values for SNAP25 similar to those of LC/A1, while LC/A4 had a 110-fold lower k_{cat} and a 2-fold higher K_m for SNAP25 than LC/A1 did (Table 2). Thus, LC/A3 and LC/A4 exhibited similar affinities for SNAP25, but LC/A4 was less efficient in the cleavage of SNAP25 relative to LC/A1. The I264R mutation in LC/A4 did not affect the K_m for SNAP25 (<2-fold difference) but increased k_{cat} to within 2-fold of that of LC/A1. This indicated that the I264R mutation influenced substrate cleavage to approach the kinetic parameters of LC/A1.

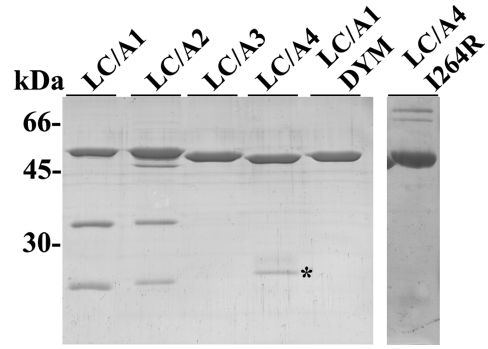

FIGURE 5: Autocleavage of LC/A subtypes. LC/A1−4 or LC/A1-Y250A,Y251A (LC/A1 DYM) (6 μM) was incubated at 37 °C for 6 h in 10 mM Tris (pH 7.6) and 20 mM NaCl. Reaction mixtures were subjected to SDS−PAGE, and autocleavage was observed following staining with Coomassie Brilliant Blue. The asterisk designates the purification background that remains constant from the 0−16 h incubation.

SNAPtide Cleavage by BoNT LCs. The commercial BoNT peptide cleavage detection assay, SNAPtide, was used as a second indication of the catalytic properties of the LC/As. SNAPtide is a fluorescent energy resonance transfer (FRET) synthetic 12-amino acid peptide, comprised of SNAP25 residues that are adjacent to the P1′ cleavage site residue (R198) (*26*). LC/A2 was 18-fold more efficient in the cleavage of SNAPtide than LC/A1 (Table 1), while LC/A3 was ~50-fold more efficient than LC/A1. This suggests that LC/A2 and LC/A3 utilize different residues in the active site to recognize SNAPtide relative to LC/A1. LC/A4 was 100-fold less efficient than LC/A1, while LC/A4-I264R had a similar efficiency for the cleavage of SNAPtide relative to LC/A1. This indicated that the I264R mutation with LC/A4 influenced the active site conformation of LC/A4, making it a more efficient LC/A for SNAPtide cleavage.

Autocatalysis of LC/A Subtypes. To further characterize the LC/A subtypes, LC/A3 and LC/A4 were examined for autocatalysis using a procedure previously described (*27*). LC/A1 and LC/A2 stimulated ~35 and ~27% autocleavage by 6 h, respectively (Figure 5), while LC/A3, LC/A4, and LC/A4-I264R did not demonstrate autocleavage, even after incubation for 16 h (data not shown). To determine the effect of pH and salt concentrations, autocatalysis assays were performed at a higher pH (8.6), a lower pH (5.5), and a higher salt concentration (250 mM NaCl). In 12 h incubations, LC/A1 showed autocatalysis under each modified condition, while LC/A3 and LC/A4-I264R did not demonstrate autocatalysis (data not shown). Each LC/A subtype possessed the dityrosine autocleavage site (*19*), which indicated that residues in addition to the cleavage site were necessary for autocleavage. Control LC (LC/A1 DYM) contained mutations to cleavage site residues (Y250A and Y251A), which abrogated autocatalysis in LC/A1 (Figure 5).

DISCUSSION

Each of the seven serotypes of the botulinum neurotoxin contains subtypes that vary in primary amino acid identity by ~3−32% (*18*). Previous genetic analysis identified two new subtypes of BoNT/A (BoNT/A3 and -A4) and demonstrated stronger homology between BoNT/A2 and -A3 than

between BoNT/A2 and -A1, while BoNT/A4 shared a stronger homology to BoNT/A1 than BoNT/A2 and BoNT/A3 (*20*). These subtypes, while identified by sequence analysis, have undergone limited characterization for catalysis, neurotoxicity, or antibody neutralization. Single changes in residues involved in substrate recognition and catalysis may circumvent the development of inhibitor strategies (*14, 18, 28*) and must be taken into consideration for inhibitor development. Antibody recognition, utilized for intoxication prophylaxis and vaccination, varies between the highly conserved BoNT/A subtypes A1 and A2 (*18, 29*). The goal of this study was to determine the catalytic properties of the LC/A for subtypes A3 and A4 to provide a better understanding of substrate recognition and cleavage.

Earlier studies showed that LC/A1 uses a pocket model for SNAP25 recognition. Breidenbach and Brunger (*17*), utilizing a crystal structure of a noncatalytic form of LC/A1 bound with SNAP25 peptide to develop a substrate recognition model for BoNT/A, proposed an α-exosite upstream of the cleavage site that affects K_m and a β-exosite downstream of the cleavage site, which primarily affects k_{cat}. Analysis of this structure suggests a number of residues on the LC in potential interaction with the SNAP25 peptide. Subsequent studies (*12*) utilized an alanine scan mutation library of SNAP25 to determine kinetically important residues on SNAP25 and point mutations on the LC to define pockets of residues on the LC necessary for interaction with SNAP25. Thus, the substrate recognition model has been refined to identify interaction sites on SNAP25 for binding (B) upstream of the active site (residues 156−183) and an active site (AS) domain (residues 187−203). The binding region for SNAP25 on LC/A1 is a band of residues wrapping around LC/A1, where interactions of residues in SNAP25 with LC/A1 have been demonstrated along the α-helix as well as the unstructured loop of SNAP25. The AS of BoNT/A1 contained clusters of residues defined by the cocrystal of LC/A1 and SNAP25 by multiple groups to interact with SNAP25 (*17, 30*). Chen et al. developed a "pocket" model for interactions between the LC/A1 and SNAP25 within the AS (*12*). The most important pocket described was the S1′ pocket, consisting of four residues (Phe 163, Phe 194, Thr 220, and Asp 370). Asp 370 has been shown, through an LC−inhibitor crystal, to be involved in stabilization of the catalytic intermediate of SNAP25 hydrolysis. Kinetic characterization by our laboratory (data not shown) showed that LC/A2 contains identical catalytic activity and undergoes autocatalysis (*31*). In contrast, BoNT/A1 and BoNT/A2 demonstrate differences with neutralizing monoclonal antibody affinities (*29*), and an increase in SNAPtide activity compared to that of LC/A1 (Table 1). This enzymatic difference is surprising, given the high level of residue identity between LC/A1 and LC/A2 (>95%), especially within known binding and catalysis residues.

LC/A3 contains the lowest level of residue identity with respect to LC/A1 within the α-exosite but is identical in the AS residues identified by Breidnebach et al. (*17*) and Chen et al. (*12*). Alternatively, LC/A4 contains residues similar to those of LC/A1 in the α-exosite binding site, with two exceptions, but contains three conserved, though sterically smaller changes at the S1′ site. Alignments of these primary protein sequences, taken with known structural and kinetic data, initially predicted a change in K_m for LC/A3 and a change in k_{cat} for LC/A4 (*19*). Kinetic data on LC/A3 did not exhibit a change in K_m compared to that of LC/A1, demonstrating that the nonconserved residue changes within the binding exosite had little effect on SNAP25 recognition. The similarity of K_m for SNAP25 by LC/A1 and LC/A3 suggests plasticity within the binding exosite for SNAP25, perhaps different interacting residues between the LC/A1 and LC/A3 for SNAP25. LC/A3 demonstrated a slightly lower activity in the linear velocity and catalytic efficiency (k_{cat}/K_m) for SNAP25. Unexpectedly, both LC/A2 and LC/A3 cleaved the synthetic substrate, SNAPtide, more efficiently than LC/A1, demonstrating incongruency between wild-type SNAP25 and SNAPtide cleavage among the LCs. The LC/A3 active site is identical in all residues recognized previously to be necessary for cleavage of wild-type SNAP25. The unexpected difference between SNAP25 and SNAPtide suggests the LCs recognize the two substrates differently. The binding exosite of SNAP25, which is not present in SNAPtide, is identical between LC/A2 and LC/A1, suggesting that SNAPtide activity differences of LC/A2 and LC/A3 compared to LC/A1 are not due to loss of the binding site. One explanation may be that in SNAPtide the P4′ residue, Lys 201, is linked by the ε-amine of the R group to DABCYL, which may block interaction with the S4′ binding pocket. The S4′ pocket consists of a single residue (E257), shown to contribute to substrate recognition and catalysis in LC/A1 (*12*). Conversely, this also suggests that since there is a shared increase in activity between LC/A2 and LC/A3 compared to that of LC/A1 in SNAPtide activity with the absence of S4′ pocket activation, residues that do not participate in the cleavage reaction of SNAP25 may now contribute to SNAPtide recognition and catalysis for LC/A2 and LC/A3. Thus, substrate recognition of SNAP25 and SNAPtide may differ for specific LC subtypes. In contrast, SNAP25 recognition is the same for LC/A1, LC/A2, and LC/A3 which suggests that upon activation of the AS by the P4′−S4′ interaction, the LC ASs are comparable. Another possibility is that since LC/A3 is identical to LC/A1 within the catalytic site, regions outside the active site residues may change the fit of SNAP25 into the catalytic site, which could account for the observed differences in cleavage rate of the SNAPtide by the different subtypes.

LC/A4 exhibited a reduced level of cleavage for SNAPtide and SNAP25. This was proposed to be due to conserved residue changes causing steric interaction differences within the putative S1′ pocket (*12, 19*). Unexpectedly, LC/A4 was inherently insoluble as a recombinant protein expressed in *E. coli*, and this property was examined as an explanation for the decrease in catalytic activity. CD spectroscopy of LC/A4 showed an α-helical pattern similar to that of LC/A1 and LC/A4-I264R, demonstrating a secondary structure similar to that of active proteins, which suggested that the change in activity was due to a subtle structural alteration via the residue substitution. A comparative hydrophobicity plot for LC/A1−4 showed two residue changes that were predicted to increase the hydrophobicity of LC/A4 versus LC/A1-A3. Examination of the LC/A1 crystal structure revealed a salt bridge between R264 and E262, which is apparently lacking in LC/A4. E263, directly adjacent to this salt bridge stabilization in LC/A1, is a conserved residue within the LC/A subtypes and is necessary for stabilization of the zinc atom within the active site during hydrolysis of

SNAP25 (*13*). Previously published studies demonstrated that conserved residue substitutions of LC/A1 at E262 decreased the k_{cat} 5-fold while retaining CD-measured secondary structure and molar ratios of zinc (*32*). This suggests that the observed decrease in activity is not due to the alignment of residue 264 that is required for optimal substrate cleavage. LC/A4-I264R demonstrated increased catalytic activity that approached that of LC/A1. One hypothesis is that substitution of Arg 264 in LC/A1 to Iso in LC/A4 destabilizes the coordination activity of E262 in relation to the zinc atom in the active site. The solubility difference between LC/A4 and LC/A4-I264R may not be due to folding differences, but to differences in protein interactions that occur after the folding process in an *E. coli* background compared to a *Clostridia* sp. background. BoNT/A4 was observed to have the I264 codon in multiple, independent overlapping DNA sequences, confirming the substitution (M. Jacobson, unpublished data). The specific toxicity of purified BoNT/A4 has not yet been demonstrated in vivo due to the difficulty of purifying the 150 kDa holotoxin from a dual-neurotoxin producing *Clostridium* sp. (W. Tepp, unpublished data).

Autocleavage is a characteristic of LC/A1 (*31*), where a dityrosine residue on the 250 loop is cleaved by active, trans-interacting LC/A1 and LC/A2. Crystal structures of the trans-interacting LC/A1 by Breidenbach and Brunger demonstrated noncanonical substrate binding and defined interacting residues on the 250 loop of both LC that were conserved within LC/A1−4. The inability of LC/A3 and LC/A4 to undergo autocleavage was not predicted, since both subtypes are highly conserved for the 250 loop and possessed the dityrosine site of cleavage. Recently, Ahmed and Smith described a number of mutations to LC/A1 in which autocatalysis was abrogated, where the mutated enzyme lost both the capacity of autocleavage and cleavage of SNAP25, coupling the two activities (*10*). The observed properties of LC/A3 and LC/A4 suggest that the capacity to undergo autocleavage and SNAP25 cleavage can also be uncoupled. Alignment of LC/A1−4 showed that the 250 loop region was conserved and did not explain the inability to recognize this self-substrate. LC/A3 contains a substitution to the loop region (N246K), which may cause a positively charged microenvironment and a loss of accessibility of this loop to the AS, while the loss of autocleavage in LC/A4 may be explained through substitutions within the S1′ pocket of the AS.

Determining differences in substrate recognition between subtypes of botulinum neurotoxin provides information for vaccine and therapies against botulism. LC/A3 and LC/A4 cleaved SNAP25 but possessed differences in catalytic efficiency and autocatalysis compared to LC/A1. These data, as well as recently published information about interacting residues of LC/A1 with SNAP25, provide a model by which LCs of other serotypes may be compared for substrate specificity and catalysis.

ACKNOWLEDGMENT

We thank the members of the Barbieri laboratory for helpful discussion.

REFERENCES

1. Shiva, G., Rossetti, O., Santucci, A., DasGupta, R. R., and Montecucco, C. (1992) Botulinum Neurotoxins are Zinc Proteases. *J. Biol. Chem. 267*, 23479–23483.
2. Binz, T., Blasi, J., Yamasaki, S., Baumeister, A., Link, E., Sudhof, T. C., Jahn, R., and Niemann, H. (1994) Proteolysis of SNAP-25 by types E and A botulinal neurotoxins. *J. Biol. Chem. 269*, 1617–1620.
3. Naumann, M., So, Y., Argoff, C. E., Childers, M. K., Dykstra, D. D., Gronseth, G. S., Jabbari, B., Kaufmann, H. C., Schurch, B., Silberstein, S. D., and Simpson, D. M. (2008) Assessment: Botulinum neurotoxin in the treatment of autonomic disorders and pain (an evidence-based review): Reports of the Therapeutics and Technology Assessment Subcommittee of the American Academy of Neurology. *Neurology 70*, 1707–1714.
4. Bandyopadhyay, S., Clark, A. W., DasGupta, B. R., and Sathyamoorthy, V. (1989) Role of the heavy and light chains of botulinum neurotoxin in neuromuscular paralysis. *J. Biol. Chem. 262*, 2660–2663.
5. Lacy, D. B., and Stevens, R. C. (1999) Sequence homology and structural analysis of the clostridial neurotoxins. *J. Mol. Biol. 291*, 1091–1104.
6. Foran, P., Lawrence, G. W., Shone, C. C., Foster, K. A., and Dolly, J. O. (1996) Botulinum neurotoxin C1 cleaves both Syntaxin and SNAP-25 in intact and permeabilized Chromaffin cells: Correlation with its blockade of Catecholamine release. *Biochemistry 35*, 2630–2636.
7. Schiavo, G., Shone, C. C., Bennett, M. K., Scheller, R. H., and Montecucco, C. (1995) Botulinum neurotoxin type C cleaves a single Lys-Ala bond within the carboxyl-terminal region of syntaxins. *J. Biol. Chem. 270*, 10566–10570.
8. Arndt, J. W., Yu, W., Bi, F., and Stevens, R. C. (2005) Crystal structure of botulinum neurotoxin type G light chain: Serotype divergence in substrate recognition. *Biochemistry 44*, 9574–9580.
9. Chen, S., Hall, C., and Barbieri, J. T. (2008) Substrate recognition of VAMP-2 by botulinum neurotoxin B and tetanus neurotoxin. *J. Biol. Chem. 283*, 21153–21159.
10. Ahmed SA, O. M., Ludivico, M. L., Gilsdorf, J., and Smith, L. A. (2008) Identification of Residues Surrounding the Active Site of Type A Botulinum Neurotoxin Important for Substrate Recognition and Catalytic Activity. *Protein J. 27*, 151–162.
11. Chen, S., and Barbieri, J. T. (2006) Unique substrate recognition by botulinum neurotoxins serotypes A and E. *J. Biol. Chem. 281*, 10906–10911.
12. Chen, S., Kim, J. P., and Barbieri, J. T. (2007) Mechanism of Substrate Recognition by Botulinum Neurotoxin Serotype A. *J. Biol. Chem. 282*, 9621–9627.
13. Rigoni, M., Caccin, P., Johnson, E. A., Montecucco, C., and Rossetto, O. (2001) Site-Directed Mutagenesis Identifies Active-Site Residues of the Light Chain of Botulinum Neurotoxin Type A. *Biochem. Biophys. Res. Commun. 288*, 1231–1237.
14. Schmidt, J. J., and Stafford, R. G. (2005) Botulinum neurotoxin serotype F: Identification of substrate recognition requirements and development of inhibitors with low nanomolar affinity. *Biochemistry 44*, 4067–4073.
15. Sikorra, S., Henke, T., Swaminathan, S., Galli, T., and Binz, T. (2006) Identification of the Amino Acid Residues Rendering TI-VAMP Insensitive toward Botulinum Neurotoxin B. *J. Mol. Biol. 357*, 574–582.
16. Arndt, J. W., Chai, Q., Christian, T., and Stevens, R. (2006) Structure of Botulinum Neurotoxin Type D Light Chain at 1.65 Å Resolution: Repercussions for VAMP-2 Substrate Specificity. *Biochemistry 45*, 3255–3262.
17. Breidenbach, M. A., and Brunger, A. T. (2004) Substrate recognition strategy for botulinum neurotoxin serotype A. *Nature 432*, 925–929.
18. Smith, T. J., Lou, J., Geren, I. N., Forsyth, C. M., Tsai, R., LaPorte, S. L., Tepp, W. H., Bradshaw, M., Johnson, E. A., Smith, L. A., and Marks, J. D. (2005) Sequence Variation within Botulinum Neurotoxin Serotypes Impacts Antibody Binding and Neutralization. *Infect. Immun. 73*, 5450–5457.
19. Arndt, J. W., Jacobson, M. J., Abola, E. E., Forsyth, C. M., Tepp, W. H., Marks, J. D., Johnson, E. A., and Stevens, R. C. (2006) A structural perspective of the sequence variability within botulinum neurotoxin subtypes A1-A4. *J. Mol. Biol. 362*, 733–742.
20. Hill, K. K., Smith, T. J., Helma, C. H., Ticknor, L. O., Foley, B. T., Svensson, R. T., Brown, J. L., Johnson, E. A., Smith, L. A., Okinaka, R. T., Jackson, P. J., and Marks, J. D. (2007) Genetic diversity among Botulinum Neurotoxin-producing clostridial strains. *J. Bacteriol. 189*, 818–832.
21. Edmond, B. J., Guerra, F. A., Blake, J., and Hempler, S. (1977) Case of infant botulism in Texas. *Tex. Med. 73*, 85–88.

22. Leighton, G. R. (1923) Botulism and Food Preservation (The Loch Maree Tragedy) Glasgow; Collins and Sons.
23. Baldwin, M. R., Tepp, W. H., Przedpelski, A., Pier, C. L., Bradshaw, M., Johnson, E. A., and Barbieri, J. T. (2008) Subunit Vaccine against the Seven Serotypes of Botulism. *Infect. Immun. 76*, 1314–1318.
24. Baldwin, M. R., Bradshaw, M., Johnson, E. A., and Barbieri, J. T. (2004) The C-terminus of botulinum neurotoxin type A light chain contributes to solubility, catalysis, and stability. *Protein Expression Purif. 27*, 187–195.
25. Fang, H., Luo, W., Henkel, J., Barbieri, J., and Green, N. (2006) A yeast assay probes the interaction between botulinum neurotoxin serotype B and its SNARE substrate. *Proc. Natl. Acad. Sci. U.S.A. 103*, 6958–6963.
26. Boldt, G. E., Kennedy, J. P., Hixon, M. S., McAllister, L. A., Barbieri, J. T., Tzipori, S., and Janda, K. D. (2006) Synthesis, characterization and development of a high-throughput methodology for the discovery of botulinum neurotoxin A inhibitors. *J. Comb. Chem. 8*, 513–521.
27. Ahmed SA, B. M., Jensen, M., Hines, H. B., Brueggemann, E., and Smith, L. A. (2001) Enzymatic autocataylsis of botulinum A neurotoxin light chain. *J. Protein Chem. 20*, 221–231.
28. Boldt, G. E., Eubanks, L. M., and Janda, K. D. (2006) Identification of a botulinum neurotoxin A protease inhibitor displaying efficacy in a cellular model. *Chem. Commun. 29*, 3063–3065.
29. Garcia-Rodriquez, C., Levy, R., Arndt, J. W., Forsyth, C. M., Razai, A., Lou, J., Geren, I., Stevens, R. C., and Marks, J. D. (2007) Molecular evolution of antibody cross-reactivity for two subtypes of type A botulinum neurotoxin. *Nat. Biotechnol. 25*, 107–116.
30. Lacy, D. B., Tepp, W., Cohen, A. C., DasGupta, B. R., and Stevens, R. C. (1998) Crystal structure of botulinum neurotoxin type A and implications for toxicity. *Nat. Struct. Biol. 5*, 898–902.
31. Ahmed, S. A., Byrne, M. P., Jensen, M., Hines, H. B., Brueggemann, E., and Smith, L. A. (2005) Enzymatic Autocatalysis of Botulinum A Neurotoxin Light Chain. *J. Protein Chem. 20*, 221–231.
32. Kukreja, R. V., Sharma, S., Cai, S., and Singh, B. R. (2007) Role of two active site Glu residues in the molecular action of botulinum neurotoxin endopeptidase. *Biochim. Biophys. Acta 1774*, 213–222.

BI801686B